



CO₂-imprinted Sustainable Carbon Derived from Sunflower Heads for Highly Effective Capture of CO₂ from Flue Gas

Wenhui Su¹, Rui Wang^{1*}, Tiansheng Zhao²

¹ School of Environmental Science and Engineering, Shandong University, Jinan 250199, China

² State Key Laboratory of High-Efficiency Utilization of Coal and Green Chemical Engineering, Ningxia University, Yinchuan 750021, China

ABSTRACT

In this work, novel and cheap CO₂ imprinted adsorbents were synthesized on the surface of activated carbon derived from sunflower heads by surface imprinting technique using ethanedioic acid and acrylamide as template molecule and functional monomer, respectively. To obtain CO₂ imprinted adsorbents with optimal properties, we studied the effects of ratio of KOH to sunflower-based activated carbon, carbon dosage and adsorption temperature, and found that the optimal conditions were alkali carbon ratio of 0.75:1, carbon dosage of 0.75 g, and adsorption temperature of 20°C. Under these conditions, maximum CO₂ adsorption capacity of the adsorbents can attain 1.71 mmol g⁻¹. The selective adsorption performance of the adsorbents for CO₂ was studied in the presence of H₂O as well as in simulated flue gas. In addition, the adsorbents after adsorption can be effectively regenerated by N₂ purge at 120°C. After five adsorption/desorption experiments, the CO₂ adsorption capacity only decreased 11%. The results showed that sustainable and cheap CO₂ imprinted adsorbents have good adsorption, selectivity and regeneration properties, which are worth being further studied and applied in CO₂ capture.

Keywords: CO₂; Selectivity; Adsorption; Imprinting technique; Biomass-derived carbon.

INTRODUCTION

With the acceleration of global industrialization, carbon dioxide emissions are increasing year by year. The data showed that the annual carbon dioxide emissions from 2015 to 2017 were 400.1, 403.3 and 405.5 ppm, respectively (Yu *et al.*, 2008; Chatterjee *et al.*, 2018; Martins *et al.*, 2018). At present, the amount of carbon dioxide in the atmospheres is nearly 50% higher than in 1750 (Yu *et al.*, 2012; Fang *et al.*, 2017; Sekiguchi *et al.*, 2018). However, there seems to be no sign of a slowdown in the growth of carbon dioxide in the atmosphere. CO₂ emitted by power, transportation and industry accounts for 39%, 23% and 22% of total emissions, respectively (Rojey *et al.*, 2005; Ciuzas *et al.*, 2016; Chen *et al.*, 2019). In the past 50 years, the global warming was mainly caused by CO₂ and expected to continue in this century (Xie *et al.*, 2017; Begum *et al.*, 2018). In view of a large amount of carbon dioxide emitted to the atmosphere, it is urgent to study advanced carbon dioxide adsorption materials for protecting the environment (Lee *et al.*, 2015; Tsay *et al.*, 2016; Chen *et al.*, 2017).

To reduce the amount of carbon dioxide in the atmosphere,

carbon capture and storage (CCS) paths provide several advantages (Wang *et al.*, 2018). CCS technology is an environmental-friendly mean for reducing atmospheric carbon dioxide from coal-fired power plants, cement production process, and iron and steel industries (Sahu *et al.*, 2017; Bhatia *et al.*, 2019). Carbon dioxide capture technology can be divided into post-combustion, pre-combustion and eutrophic combustion (Leung *et al.*, 2014). Post-combustion (Huang *et al.*, 2016), pre-combustion (Naderi *et al.*, 2019) and eutrophic combustion (Pan *et al.*, 2015) process routes can easily follow the existing separation process and energy conversion process (Plaza *et al.*, 2007). In the traditional post-combustion process, however, carbon dioxide is separated from flue gases, which is accompanied by high energy consumption (Merkel *et al.*, 2010). In order to solve this problem, scholars developed a series of adsorbents to capture CO₂ (Li *et al.*, 2013), such as zeolite (Zhang *et al.*, 2014), silica (Yang *et al.*, 2013), activated carbon (Li *et al.*, 2010), ordered porous carbon (Chew *et al.*, 2010) and other carbon-containing materials (Wickramaratne *et al.*, 2013). Kim *et al.* (2019) synthesized the K-Cha zeolite microspheres containing strontium by one-step template-free hydrothermal method, the K-Cha molecular sieves microspheres showed grading characteristics, good adsorption performance for water (316 cm³ g⁻¹) and carbon dioxide (167.0 mg g⁻¹, 10 bar) at 298 K. And the adsorption selectivity factor of CO₂/N₂ was 10 (Kim *et al.*, 2019). Jiang *et al.* (2019) studied the CO₂

* Corresponding author.

E-mail address: wangrui@sdu.edu.cn

adsorption properties of activated carbon, the commercial adsorbent (i.e., monoethanolamine) and chemical adsorbent (i.e., polyethyleneimine/silica) in order to assess the post-combustion capture advantages for carbon dioxide. The results showed that polyethyleneimine/silica and activated carbon exhibited higher net efficiency of CO₂ capture than monoethanolamine. They found that the regeneration heat of activated carbon was higher than those of monoethanolamine and polyethyleneimine/silica, but it could be reduced through increasing the CO₂ concentration. However, the current materials still have limitations in adsorption properties, adsorption conditions and selectivity (Wang *et al.*, 2011).

Imprinting technology (IT) is a biomimetic molecular recognition technology that simulates the recognition mechanism of enzyme-substrate and antibody-antigen molecules in nature (Liu *et al.*, 2008). According to the type of targets, IT can be divided into two categories: molecular imprinting technology (MIT) and ion imprinting technology (Huang *et al.*, 2018). Based on IT, scholars developed a series of functional adsorbents with special recognition and strong adsorption abilities for targets. Generally, the preparation processes of molecular imprinting polymers (MIPs) with recognition ability are shown in Fig. 1 (Wang *et al.*, 2019): First, select reasonable functional monomers (Zhang *et al.*, 2012) to form pre-polymers with templates by covalent, non-covalent or semi-covalent way (Pan *et al.*, 2010); second, cross-linkers and initiators are used to initiate the chemical polymerization reaction to form stable polymers under certain conditions (Nabavi *et al.*, 2017); Finally, the templates are removed by extraction or acid elution to obtain MIPs with recognition sites for targets (Li *et al.*, 2010; Wang *et al.*, 2010). In addition, choosing appropriate template molecule is extremely significant for its adsorption ability in the preparation of MIPs. Typically, the target material is chosen

as a template molecule. However, when the target material is unstable and has low-solubility in the polymerization system, it cannot be used as the template molecule directly. Therefore, the substitution template method is used to prepare MIPs through choosing the template molecule similar to that of target substance (Huang *et al.*, 2019).

At present, scholars have widely studied the preparation methods and applications of MIPs. In order to improve the diffusion kinetics, Xu *et al.* (2019) used surface imprinting technique to prepare MIPs on the surface of mesoporous silica materials. The kinetic experiments showed that the method could effectively improve the mass transfer rate. Zhao *et al.* (2014) studied the carbon dioxide separation of molecular imprinted adsorbent from the coal-fired flue gas after desulfurization. The results showed that the NO in flue gas had minor effects on the adsorption performance of the adsorbents for carbon dioxide, and the adsorbents had good adsorption performance and selectivity. With the development of molecular imprinting technology, some new elements have been introduced into molecular imprinted polymers.

Traditional activated carbon has high mechanical strength, fast adsorption speed, high purification degree, and long service life, but the adsorption of gas is affected by its specific surface area and pore size distribution. The traditional activated carbon has a small specific surface area and a wide pore distribution, and the pore volume of the micropores that can effectively capture CO₂ is small, resulting in a low adsorption amount. Compared with biomass-based activated carbon, the pore structure of activated carbon can be effectively adjusted according to the characteristics of CO₂ molecules, resulting in a significant increase in the amount of CO₂ adsorption. Biomass-based carbons are a kind of cheap, sustainable and resourceful material with unique structures (Chen *et al.*, 2016). They have excellent stability and

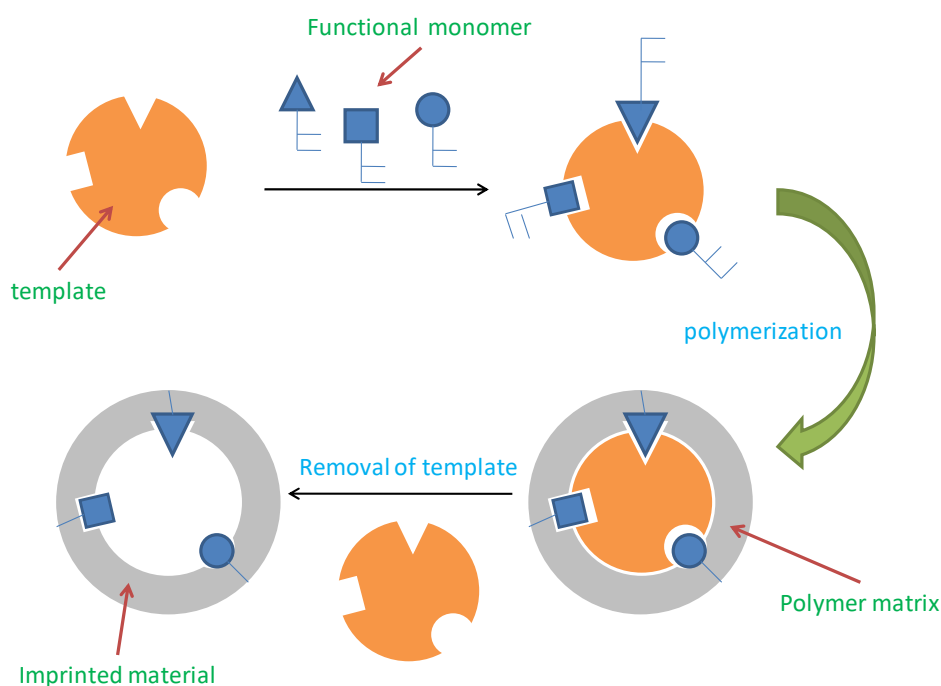


Fig. 1. Schematic representation of the imprinting process.

regeneration performance, and their pore structure is easy to design. The original biochar itself is highly non-porous and exhibits low CO₂ adsorption capacity due to low specific surface area and pore volume (Alabadi *et al.*, 2015). To enhance its adsorption performance, the specific surface area and pore volume can be increased by chemical activation at moderate or high temperatures. Therefore, activated biochar is formed by activation of biomass carbon, and these materials exhibit better CO₂ adsorption capacity (Singh *et al.*, 2017). Many researchers preferred to use a variety of plant residues such as coconut shell (Jain *et al.*, 2015), corn-straw (Chi *et al.*, 2017), rice husks (Kizito *et al.*, 2015) and peanut straw (Shi *et al.*, 2018). Among them, sunflower is a lignin-rich biomass with rich net structures. In the sunflower harvest season, a large number of sunflower heads are discarded. To avoid the waste of resources and relieve the treatment pressure of solid wastes, an activated carbon based on sunflower heads as carbon sources was prepared in this work. Table 1 shows the comparison of adsorption capacity of different activated carbon adsorbents. Singh *et al.* (2019) describe a simple one-step method that uses porous D-glucose to prepare activated porous carbon spheres to capture carbon dioxide by using a new non-corrosive chemical, i.e., potassium acetate. We use activation methods to control chemical structure, morphology, porosity, and texture characteristics, while Singh works by changing the amount of potassium acetate. The strategies used to synthesize these materials are simple and the total cost of precursors and processes is low. It is speculated that a similar activation strategy can be used to prepare a series of porous activated carbons with enhanced properties and use different carbon precursors for various energy and environmental applications. Active carbon adsorption of CO₂ is a typical physical adsorption. Adsorption refers to the accumulation of components at the phase interface when a fluid is in contact with a porous medium. This article discusses the phenomenon of solid adsorption of gases. The solid matter is called an adsorbent, and the adsorbed gaseous substance is called an adsorbate. An adsorbed phase is formed between the solid adsorbent and the adsorbed gas molecules. For activated carbon adsorption of carbon dioxide, it is caused by the attractive force between the adsorbate carbon dioxide molecules and the adsorbent activated carbon, but this binding force is relatively weak and easy to desorb.

In this work, surface imprinting technology was used to prepare CO₂-MIPs with highly selective properties for CO₂

using the self-prepared carbon as the carrier that were prepared by using waste biomass sunflower heads as carbon sources. The adsorption properties of carbon dioxide under different conditions were investigated, and the preparation methods and adsorption conditions were optimized. The CO₂-MIPs were characterized by scanning electron microscopy, nitrogen adsorption/desorption test, fourier transform infrared spectroscopy and thermogravimetric analysis.

EXPERIMENTS

Chemical Reagent

Oxalic acid was purchased from Kangde Chemical Co., Ltd. (Laiyang, China). Acrylamide (AAM), toluene and hydrochloric acid were purchased from China Pharmaceutical Group Chemical Reagent Co., Ltd. Ethylene glycol dimethyl acrylate (EGDMA), azodiisobutyronitrile (AIBN) were purchased from Shanghai Macklin Biochemical Co., Ltd. Acetonitrile (AN) and methanol were purchased from Fuyu Fine Chemical Co., Ltd. (Tianjin, China). The purity of all gases used in this work is higher than 99.99%, which is provided by Qingdao Hausen New Energy Co., Ltd.

Synthesis of Activated Carbon

Carbonization

The sunflower heads screened (4 g) were put into tubular furnace and carbonized according to the following heating procedure: the material was purged with N₂ for 30 min at room temperature, heated to 773 K at a heating rate of 5 K min⁻¹, and kept for 90 min at 773 K. Finally, the material was cooled naturally to room temperature. N₂ protection was used throughout during the carbonization process.

Activation

Carbonized material (1 g) was impregnated in 20 mL distilled water with KOH (0.75 g) at room temperature for 48 h. The impregnated material was dried in oven at 378K. The dried material was activated by the following heating procedure: the material was purged with N₂ for 30 min at room temperature, raised to 773 K at the rate of 10 K min⁻¹, then raised to 973 K at the rate of 5 K min⁻¹ and maintained for 2 h. The activation process was protected by N₂. The purpose of activation is to further increase the specific surface area of the materials, and form numerous channels on the basis of the pore structure of the carbonized materials.

Table 1. Comparison of different adsorbents.

Order	Sorbents	Adsorption capacity	References
1	carbon sphere (CS)	1.12 cm ³ g ⁻¹	Wickramaratne <i>et al.</i> (2013)
2	granular activated carbon (GAC)	24.9 mg g ⁻¹	Lu <i>et al.</i> (2008)
3	activated biocarbon	1.67 mmol g ⁻¹	Serafina <i>et al.</i> (2019)
4	activated carbon	8.5 mol kg ⁻¹	Siriwardane <i>et al.</i> (2001)
5	molecular sieve 13X	5.2 mol kg ⁻¹	
6	molecular sieve 4A	4.8 mol kg ⁻¹	
7	carbon composite	0.73 mmol g ⁻¹	Thiruvenkatachari <i>et al.</i> (2013)
8	PECONF	1.9 mmol g ⁻¹	Mohanty <i>et al.</i> (2011)
9	CO ₂ -MIPs	1.71 mmol g ⁻¹	this work

Synthesis of CO₂-MIPs

MIPs adsorbent was synthesized by the following process: 3 mmol ethylene glycolic acid and 12 mmol AAM were dissolved in 80 mL mixed solution of AN and toluene (1:1, v/v). After stirring for 30 min, 20 mmol EGDMA and 0.3 mmol AIBN were added into the mixture. Then, the mixture was dispersed by ultrasonic device for 15 min and purged by N₂ for 10 min to remove oxygen. After that, the mixture was sealed and stirred at 60°C for 12 h. The polymer was washed three times with HCl/methanol (1:9, v/v) solution to remove unreacted substances and then filtered out. The obtained polymer particles were washed with distilled water to neutrality and dried in 60°C oven.

Adsorption Experiment

Basic Experiments

In this paper, the performance of adsorbent was evaluated by a fixed bed dynamic adsorption device. The adsorption test device is shown in Fig. 2. The prepared adsorbent (0.5 g) was filled into the glass adsorption column (10 mm diameter; 5 mm inner diameter). At the bottom of the column, there is a gas distribution orifice plate with a pore diameter of about 100 μm. Before adsorption, the CO₂-MIPs were treated by the N₂ flow of 500 mL min⁻¹ (about 1 h) at 98°C to release CO₂ adsorbed on the adsorbent. After the experiment started, 10% CO₂ was kept in the adsorption column at 25°C at a flow rate of 10 mL min⁻¹, and the gas coming out was mixed with N₂ (90 mL min⁻¹). Desorption experiments were performed after adsorption experiments. During the adsorption process, the gas flow rate was controlled by mass flow controller (D08-3D/ZM), and the CO₂ concentration was measured by portable infrared CO₂ analyzer (GXH-3010E). In addition, desorption experiments were carried out under

120°C in N₂ flow to remove adsorbed CO₂.

In order to reuse the adsorbent and collect the captured carbon dioxide, we carried out desorption experiments. After CO₂ adsorption becomes saturated, the material is desorbed under high temperature and N₂ purging to ensure multiple utilization. CO₂ desorbed by this method is collected together with N₂. In the desorption process, we use mass flowmeter to control the flow rate of N₂.

The adsorption capacity of CO₂ (q_b) was calculated according to the following equation:

$$qb = \int_0^t (C_{inlet} - C_{outlet}) V / (22.4m) dt \quad (1)$$

where, t (min) is the adsorption time, C_{outlet} (% vol) is the concentration of CO₂ after CO₂-MIPs adsorption, C_{inlet} (% vol) is the initial concentration of CO₂, V (mL min⁻¹) is the flow of gas into the adsorbent; and m (g), the mass of the adsorbent.

Contrast Experiments

In the six groups of contrast experiments as shown in Table 2, the research factors are as follows: alkali-carbon ratio, dosage of the carrier, adsorption temperature, desorption temperature, concentration, water and selectivity. By comparing the adsorption curves of six group experiments, the optimum operation conditions were obtained.

Characterization

The pattern of the MIPs was characterized by Japanese electron JEOL-7500F field emission scanning electron microscopy (FESEM). The surface properties and chemical structures of the adsorbents were studied by Brookvertex

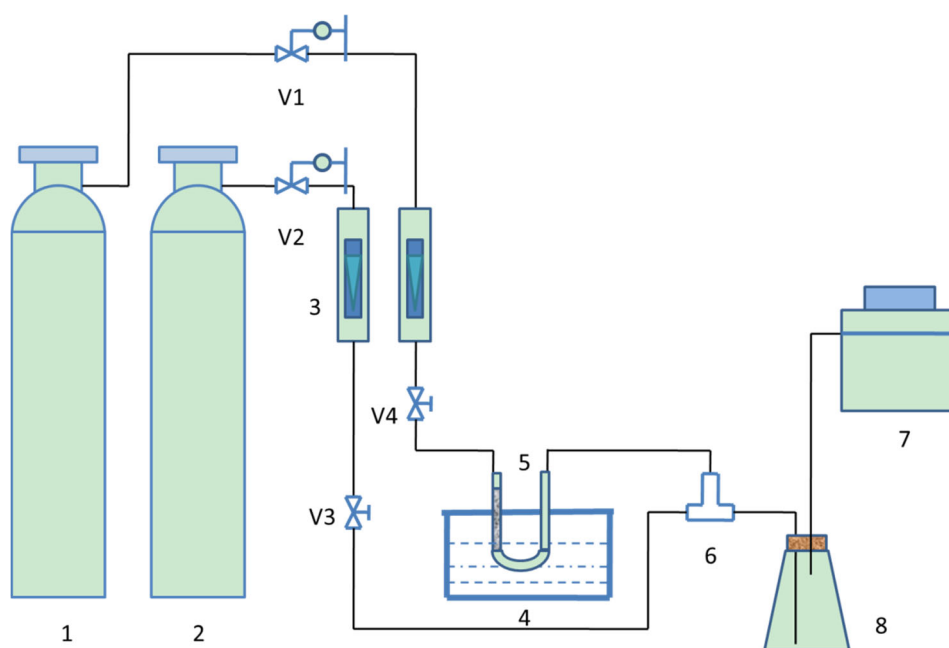


Fig. 2. Diagram of experimental apparatus for adsorption: (1) CO₂/N₂ cylinder; (2) N₂ cylinder; (3) mass flow meter; (4) water bath; (5) adsorption tube; (6) three-way pipe; (7) CO₂ analyzer; (8) mixed cylinder; V1, V2 pressure reducing valves; V3, V4 shutoff valves.

Table 2. Operation conditions of experiments.

Experiments	Ratio of alkali to carbon (g g ⁻¹)	Dosage of the Carrier (g)	Adsorption temperature (°C)	Desorption temperature (°C)	Concentration of CO ₂ (%)	H ₂ O vapor
basic	0.75	0.75	25	120	10	without
1	0.25	0.75	25	120	10	without
	0.5	0.75	25	120	10	without
	0.75	0.75	25	120	10	without
	1	0.75	25	120	10	without
	0.75	0	25	120	10	without
2	0.75	0.5	25	120	10	without
	0.75	0.75	25	120	10	without
	0.75	1	25	120	10	without
	0.75	0.75	25	120	10	without
3	0.75	0.75	25	120	10	without
	0.75	0.75	50	120	10	without
	0.75	0.75	75	120	10	without
4	0.75	0.75	25	80	10	without
	0.75	0.75	25	100	10	without
	0.75	0.75	25	120	10	without
	0.75	0.75	25	140	10	without
5	0.75	0.75	25	120	1	without
	0.75	0.75	25	120	4	without
	0.75	0.75	25	120	7	without
	0.75	0.75	25	120	10	without
6	0.75	0.75	25	120	10	with
	0.75	0.75	25	120	10	without

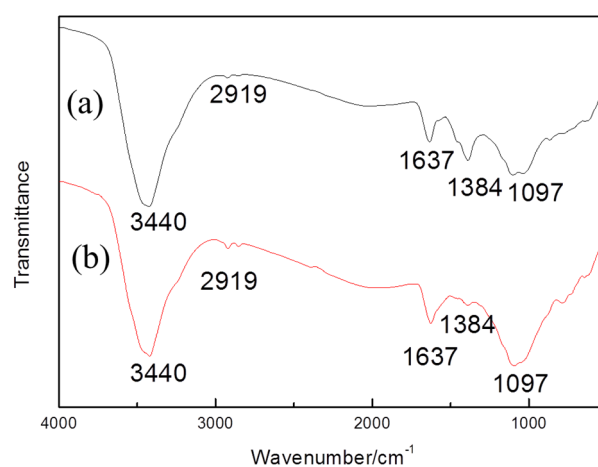
70 fouriertransform infrared spectrometer (FT-IR). The thermal stability of the adsorbents was analyzed by using Netzsch 209F3 thermogravimetric analyzer (TG) at the heating rate of 10°C min⁻¹ in nitrogen atmosphere. Mac ASAP 2020 automatic physical adsorption analyzer was used to measure the specific surface area and pore size distribution of the MIPs with nitrogen.

RESULTS AND DISCUSSIONS

Structural Characterization

Fig. 3 shows the FT-IR spectra of the carrier and CO₂-MIPs. The broad bands near 3440 cm⁻¹ are the stretching vibration of OH group in -COOH and -C-OH. The absorption peaks near 1637 cm⁻¹ are caused by the superposition of the deformed vibration of N-H bond and the stretching vibration of C=O. The absorption peaks at 1384 cm⁻¹ and 1097 cm⁻¹ are the stretching vibration of C-N. The infrared spectra of the two adsorbents are nearly the same, indicating that their chemical groups are basically similar.

Fig. 4 shows the nitrogen adsorption-desorption isotherms and pore size distributions of the carrier and CO₂-MIPs. According to Brunauer-Deming-Teller classification, the curves belong to type I isotherm, indicating that CO₂-MIPs were mainly composed of microporous structure. With the increase of relative pressure, the adsorption curve exhibited hysteresis. From the pore distribution curve, the pore size distribution of CO₂-MIPs was concentrated. The specific surface area, pore volume and pore diameter are shown in Table 3. The specific surface area of CO₂-MIPs was higher than that of the carrier. Pore volume and pore size of CO₂-MIPs

**Fig. 3.** FT-IR spectra of the (a) carrier and (b) CO₂-MIPs.

were smaller than those of carrier. This shows that the macropores of the carrier decreased after molecular imprinted polymerization, and its micropores and mesopores increased, leading to the decrease in average pore size.

Fig. 5 shows the SEM images of the carrier and CO₂-MIPs. Compared with the SEM image of the carrier, the CO₂-MIPs obviously exhibits more pores, illustrating that surface imprinting technology played the role in creating more adsorption cavities. Combined with the structure analysis of BET measurement, it can be concluded that the micropore and mesopore of CO₂ imprinted activated carbon increased significantly, which is beneficial to CO₂ adsorption in theory.

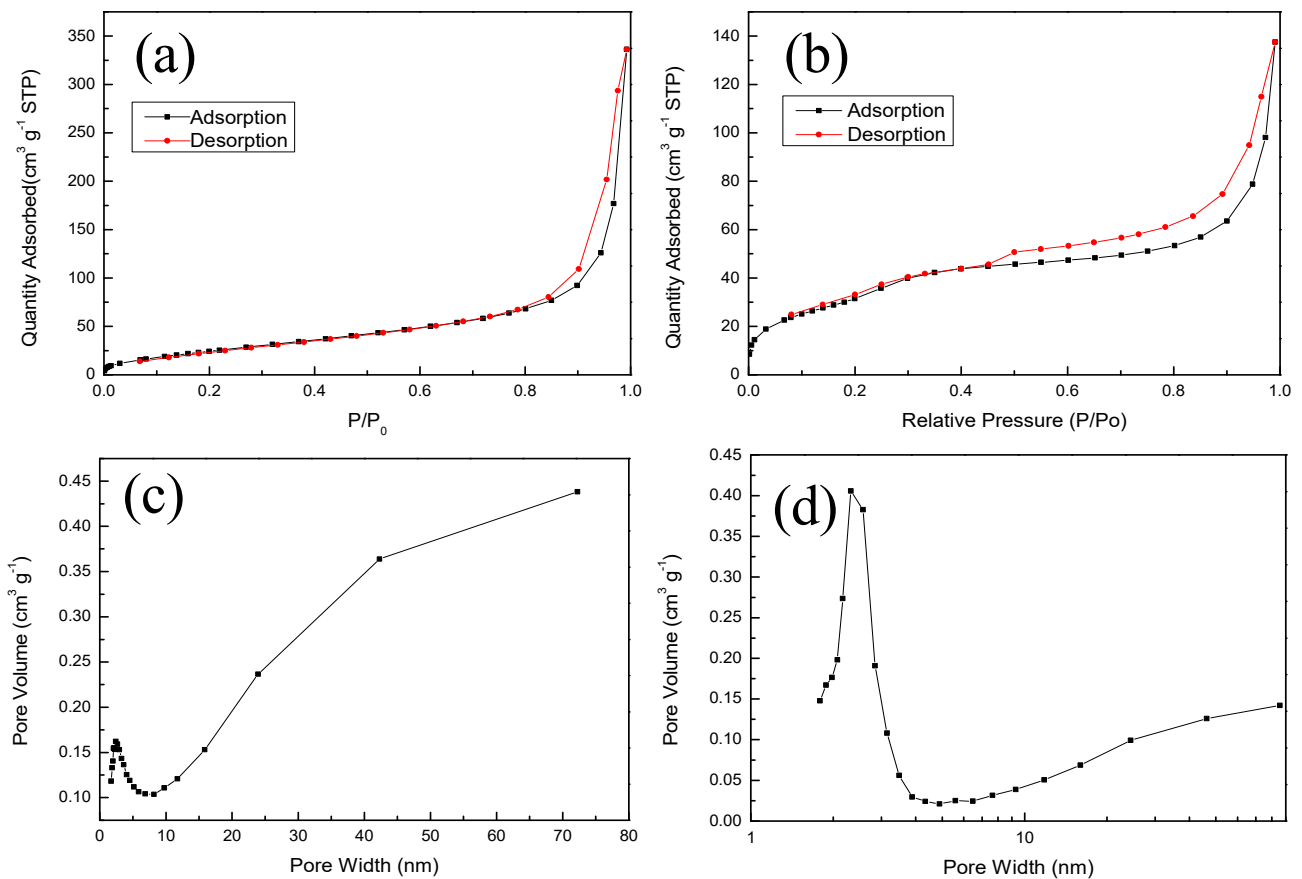


Fig. 4. N₂ adsorption/desorption curves of the (a) carrier and (b) CO₂-MIPs; pore size distribution of the (c) carrier and (d) CO₂-MIPs.

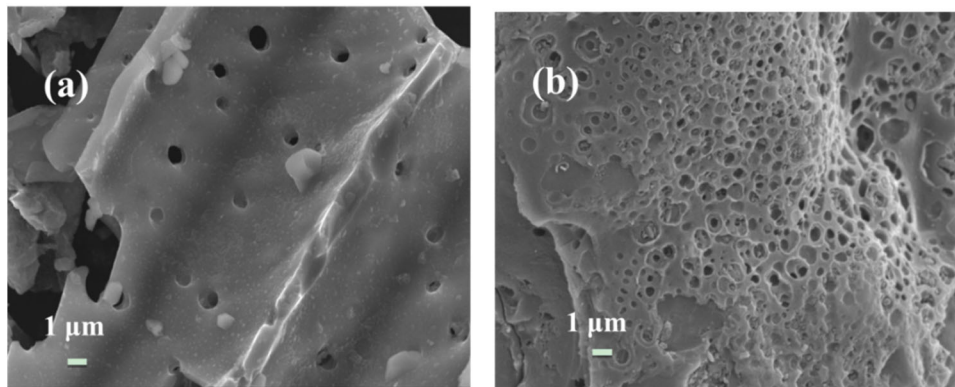


Fig. 5. FESEM of the (a) carrier and (b) CO₂-MIPs.

Fig. 6 shows the thermogravimetric analyses of the carrier and CO₂-MIPs. It can be seen from the diagram that the weight of CO₂-MIPs exhibits less decline in comparison with that of the carrier during heating from room temperature to 800°C. The weight of the carrier decreases by 3.44% from room temperature to 100°C, which was caused by desorption of H₂O that was physically adsorbed on the surface of the carrier, while the weight of CO₂-MIPs decreases by 2.94% before 158°C. Under N₂ protection, when the temperature rises from 158°C to 800°C, the weight loss of the carrier is 10.4%, while that of the CO₂-MIPs is

only 7.55%. According to the above experimental results, it can be found that the stability of CO₂-MIPs is better than that of the carrier, indicating that the imprinting process is conducive to the formation of structurally stable adsorbent.

Investigation on Preparation Conditions

The ratio of alkali to carbon is an important factor in the preparation of sunflower-based activated carbon, which has a great influence on the pore structure of activated carbon. Fig. 7 is the adsorption curves of CO₂ on different carriers prepared using different alkali-carbon ratios. With the increase

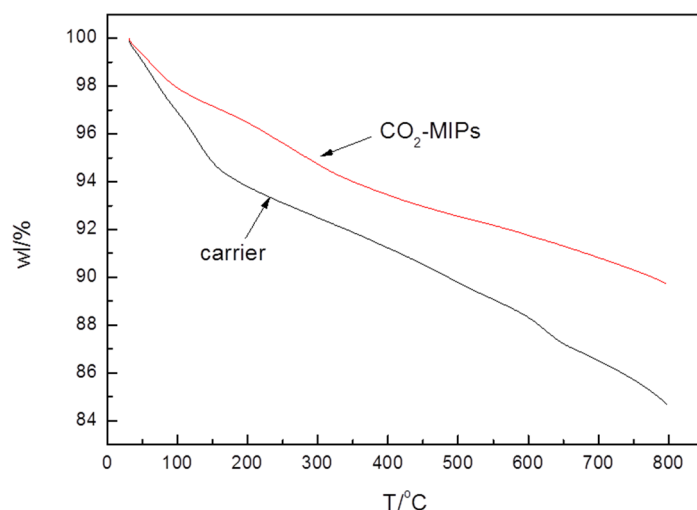


Fig. 6. Thermal decomposition of the carrier and CO₂-MIPs.

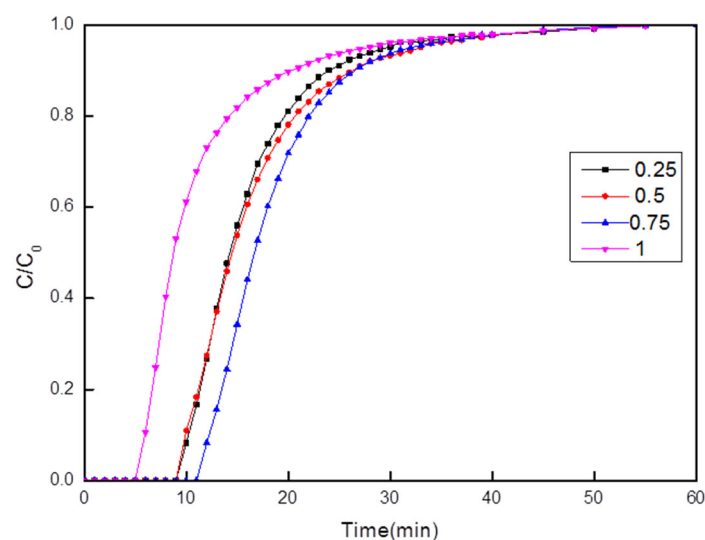


Fig. 7. The adsorption curves under different ratio of alkali to carbon.

of the ratio of alkali to carbon, the CO₂ adsorption amount of sunflower-based activated carbon increases first and then decreases. When the ratios of alkali to carbon are 0.25:1, 0.5:1, 0.75:1 and 1:1, the adsorption capacities were 1.28, 1.31, 1.45 and 0.90 mmol g⁻¹, respectively. The maximum adsorption capacity was obtained when the ratio of alkali to carbon was 0.75:1. The results show that low alkali-carbon ratio leads to inadequate activation and less pore structure, while high alkali-carbon ratio leads to excessive activation and the damage of pore structure, both of which are not conducive to improve adsorption capacity of the sunflower-based activated carbon for CO₂.

Fig. 8 is the CO₂ adsorption curves of CO₂-MIPs prepared with different dosages of the carriers in the preparation process. In order to enhance the interaction between CO₂ and the carrier, a large number of CO₂ trapping sites were created on the surface of the carrier through MIT to obtain CO₂-MIPs. When the dosages of the carriers were 0, 0.5, 0.75 and 1 g, the adsorption capacities of CO₂-MIPs reached

0.76, 1.03, 1.39 and 1.29 mmol g⁻¹, respectively. The best adsorption capacity was obtained when the dosage of the carrier was 0.75 g. When the dosage of the carrier is too low, the accumulation of active sites led to the decrease of utilization rate of adsorption sites. When the adding amount is too high, the removal efficiency is also low, which may be due to the average adsorption sites in per gram CO₂-MIPs decrease.

Effects of Operation Conditions

Fig. 9 shows the adsorption curves of CO₂-MIPs for CO₂ at different temperatures. With the increase of temperature, the adsorption capacity of CO₂ on CO₂-MIPs decreases gradually, indicating that the CO₂ adsorption is a weak interaction, which is significantly affected by temperature. The best CO₂ adsorption temperature of CO₂-MIPs was achieved at 25°C. The reason is that the binding affinity of CO₂-MIPs for CO₂ gradually decreases as the temperature increases, leading to that some adsorbed CO₂ was desorbed

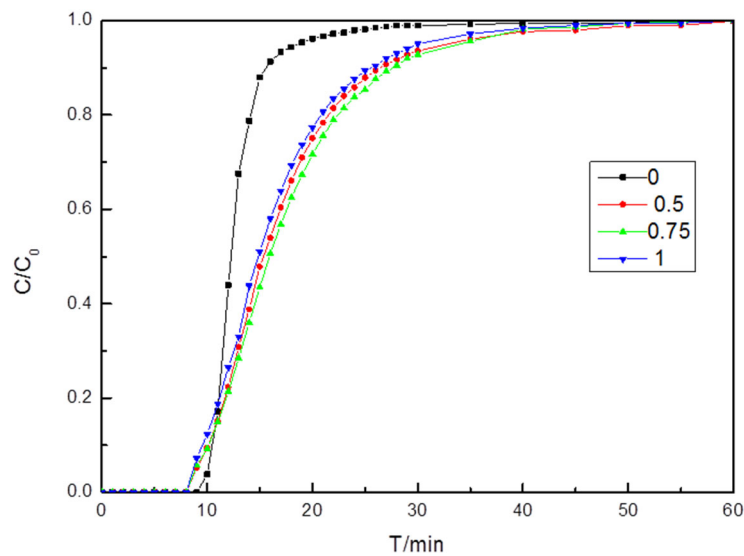


Fig. 8. The adsorption curves of CO₂-MIPs prepared with different dosages of the carrier.

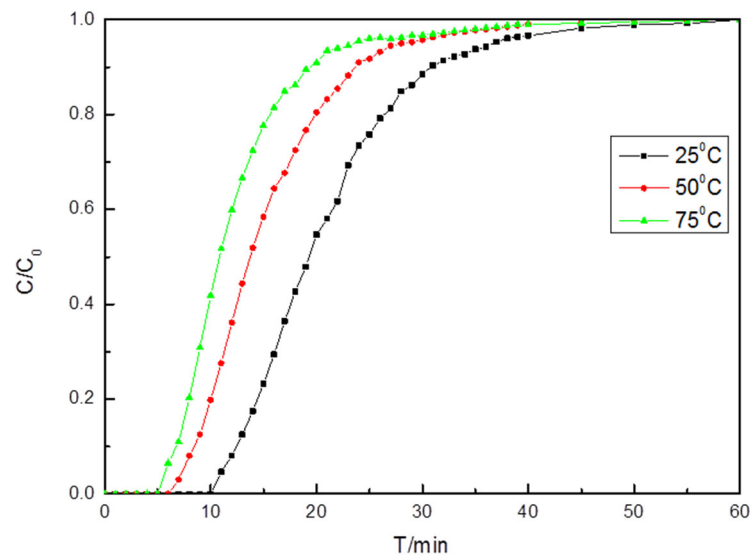


Fig. 9. The adsorption curves obtained under different temperatures.

from the adsorbent. Therefore, the temperature increase promotes CO₂-MIPs to quickly reach the adsorption equilibrium with comparatively lower CO₂ adsorption saturation capacity.

In Fig. 10, the CO₂ adsorption rate depends considerably on CO₂ concentration. When the CO₂ concentrations in the flue gas are 1%, 4%, 7% and 10%, the CO₂ adsorption capacities of the CO₂-MIPs are 2.52, 2.06, 1.71 and 1.39 mmol g⁻¹, respectively. The results showed that the lower concentration of CO₂ in the feed gas had the better adsorption effect.

Fig. 11 shows the adsorption curves of CO₂-MIPs regenerated at different temperatures. When the regeneration temperature of CO₂-MIPs was 120°C, the CO₂ adsorption capacity of the regenerated CO₂-MIPs reached the maximum, indicating that the regenerated CO₂-MIPs at 120°C exhibited the best reusability. From the above, the optimum desorption temperature is 120°C. Fig. 12 shows the variation of

saturated adsorption capacity of CO₂-MIPs during cyclic adsorption/desorption experiments. The saturated adsorption capacity of CO₂-MIPs after first regeneration exhibits a slight decrease, which is due to the incomplete regeneration of the partial adsorption sites of CO₂-MIPs at 120°C. In the subsequent cyclic experiments, the CO₂ adsorption capacity tends to be stable. After 5 cycles, the CO₂ adsorption capacity of the regenerated CO₂-MIPs has a little decrease. The reason is that part of CO₂ adsorbed in the micropore of the adsorbent has strong chemical interaction with the adsorbent, which makes it difficult to desorb, resulting in the decrease of the adsorption capacity of CO₂-MIPs.

Fig. 13 shows the CO₂ adsorption curves under the relative humidity of 70% in comparison with dry gas. The CO₂ adsorption capacities of CO₂-MIPs in the presence and absence of H₂O vapor were 1.40 and 1.44 mmol g⁻¹, respectively, illustrating that humidity has no remarkable

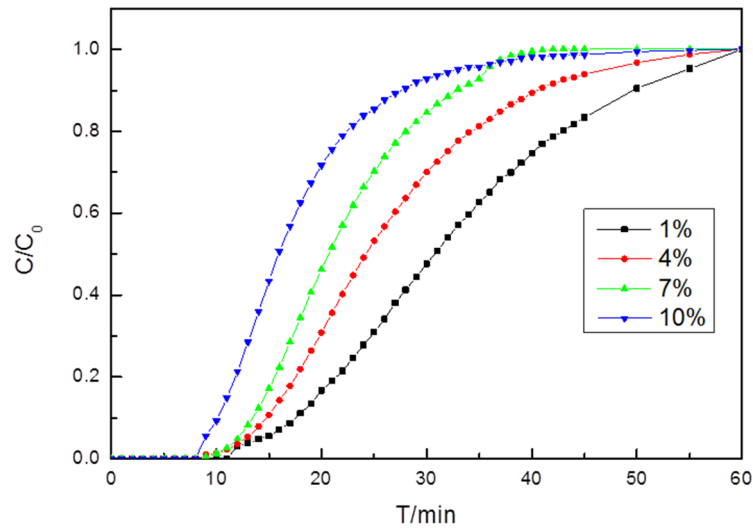


Fig. 10. The adsorption curves obtained under different content of CO₂.

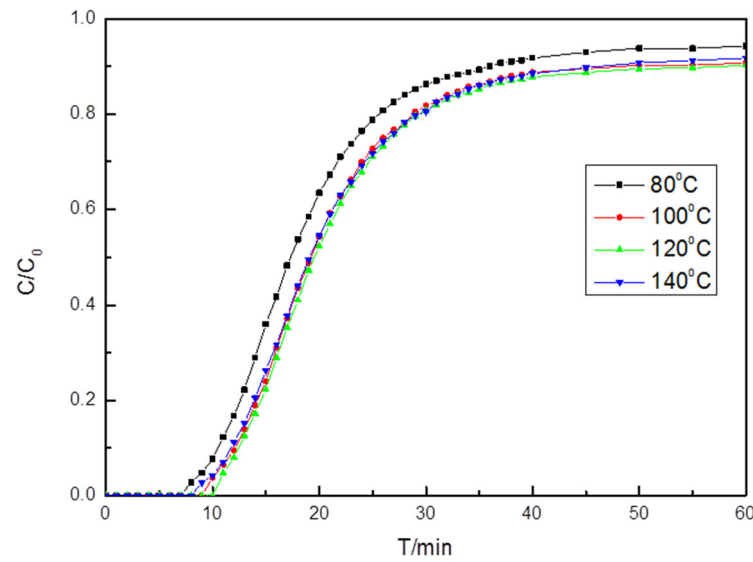


Fig. 11. The adsorption curves obtained under different desorption temperatures.

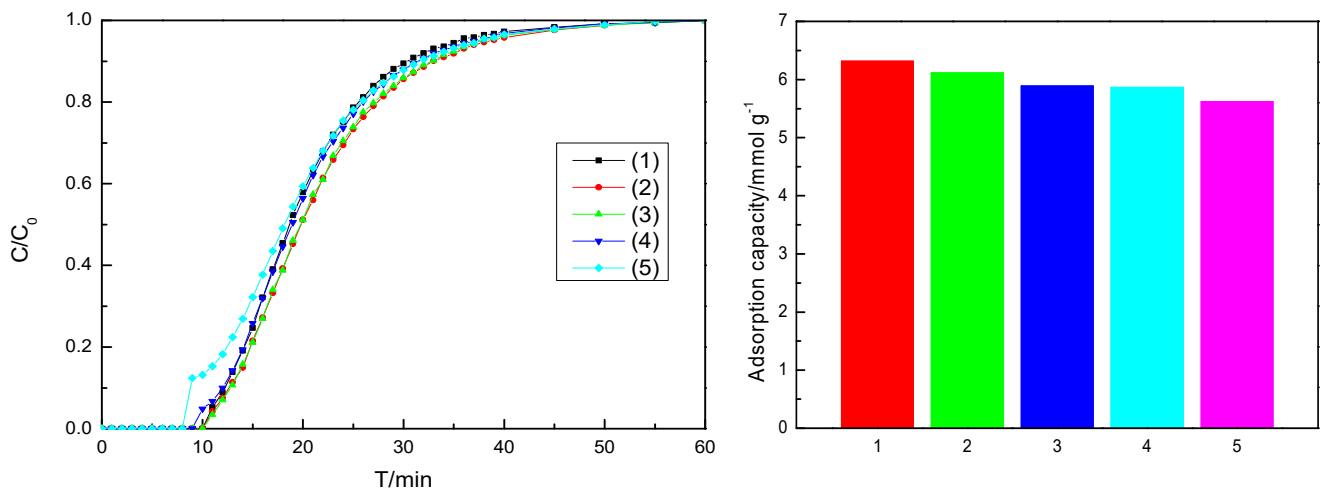


Fig. 12. Performance of CO₂-MIPs during adsorption/desorption cycle.

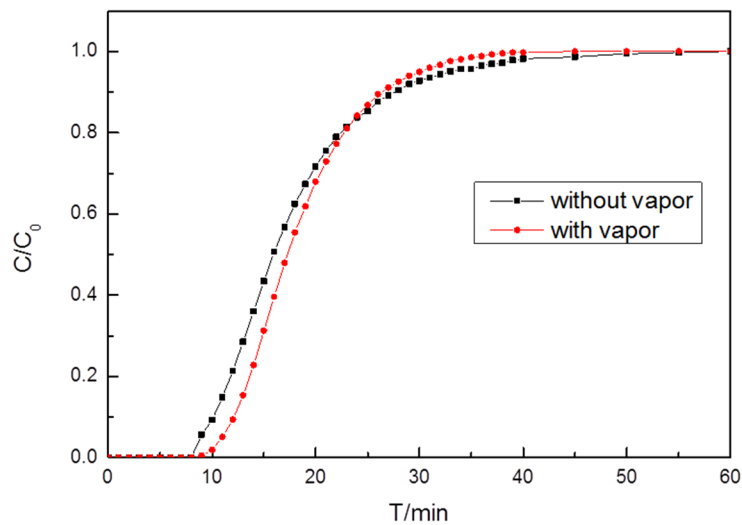


Fig. 13. The adsorption curves obtained with or without vapor.

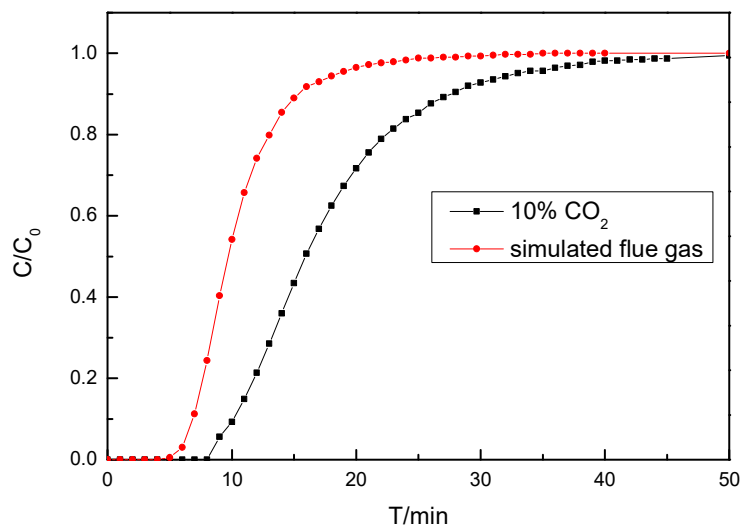


Fig. 14. The adsorption curves under the conditions of simulated flue gas.

influence on the CO₂ adsorption capacity of CO₂-MIPs. The results can be explained by the surface properties of CO₂-MIPs and the mechanism of CO₂ adsorption. There are a large amount of amino active sites on the surface of CO₂-MIPs, which play an important role in increasing the interaction between CO₂ and CO₂-MIPs. In theory, amide groups can interact with water molecules. However, hydrogen bonds between water molecules weaken the interaction between amide groups and water molecules. In addition, CO₂ molecule is non-polar, and the hydrophobic group has little effect on the interaction between CO₂ molecule and amide group. Compared with the activated carbon aerogel amine adsorbent, when water is involved in the reaction, the carbamate formed by the reaction of carbon dioxide and amino acid will continue to react with carbon dioxide and water molecules, thus forming bicarbonate. The amino group in organic amines will also react with CO₂ and water molecules to form bicarbonate, which will increase the amount of CO₂ adsorption.

Selectivity

Under the optimal operating conditions, we compared the adsorption capacity of CO₂-MIPs in the atmosphere of 10% CO₂ and simulated flue gas, including CO₂ (10%), N₂ (89.92%), SO₂ (350 mg m⁻³), NO (500 mg m⁻³). As shown in Fig.14, the CO₂ adsorption capacity of CO₂-MIPs in simulated flue gas is to some extent lower than that in N₂ diluted CO₂, but the difference is within acceptable level. Apparently, the basic and acid groups loaded on the surface of carbon materials can actually uptake other gaseous species, and the porous structure of activated carbon is also conducive to other competitive adsorptions.

CONCLUSION

Porous carbon materials were prepared by using abandoned sunflower heads as a carbon source, and cheap CO₂-MIPs were prepared by using sunflower-based activated carbon as carrier. The CO₂ adsorption performance

of CO₂-MIPs was investigated. The following conclusions were drawn:

- (1) CO₂ adsorption performance of the carrier can be improved by changing the dosage of activator (KOH), and the optimum ratio of alkali to carbon was 0.75:1.
- (2) By changing dosage of the carrier in the preparation process of CO₂-MIPs, we found the CO₂-MIPs had the best adsorption capacity when the dosage of the carrier was 0.75 g.
- (3) The effect of temperature on the MIPs adsorbent is remarkable. With the increase of temperature, the adsorption capacity of CO₂ on adsorbents decreases gradually. 25°C is the best adsorption temperature for CO₂-MIPs.
- (4) The optimum desorption temperature was 120°C, and the CO₂ adsorption capacity of regenerated CO₂-MIPs can reach 1.91 mmol g⁻¹. During the five adsorption/desorption cycles of CO₂-MIPs, the adsorption capacity has a slight decrease.
- (5) While water vapor has no remarkable influence on CO₂ adsorption capacity of CO₂-MIPs, the competitive adsorbates in simulated flue gas may to some extent weaken CO₂ adsorption.

As a whole, CO₂-MIPs developed in this work have ideal adsorption performance and are worth further studying and integrating into industrial treatment unit.

ACKNOWLEDGMENTS

This work was supported by the National Natural Science Foundation of China (Nos. 21276144, 21511130021), the Key Research and Development Program of Shandong Province, China (2017GSF217006), the PetroChina Innovation Foundation (No. 2013D-5006-0507), and the Foundation of State Key Laboratory of High-efficiency Utilization of Coal and Green Chemical Engineering (No. 2017-K30).

REFERENCES

- Alabadi, A., Razzaque, S., Yang, Y., Chen, S. and Tan, B. (2015). Highly porous activated carbon materials from carbonized biomass with high CO₂ capturing capacity. *Chem. Eng. J.* 281: 606–612.
- Begum, B. and Hopke, P. (2018). Ambient air quality in Dhaka Bangladesh over two decades: Impacts of policy on air quality. *Aerosol Air Qual. Res.* 18: 1910–1920.
- Bhatia, S., Bhatia, R., Jeon, J., Kumar, G. and Yang, Y. (2019). Carbon dioxide capture and bioenergy production using biological system- A review. *Renewable Sustainable Energy Rev.* 110: 143–158.
- Chatterjee, A., Roy, A., Chakraborty, S., Karipot, A., Sarkar, C., Singh, S., Ghosh, S., Mitra, A. and Raha, S. (2018). Biosphere atmosphere exchange of CO₂, H₂O vapour and energy during spring over a high altitude Himalayan forest in Easter India. *Aerosol Air Qual. Res.* 18: 2704–2719.
- Chen, J., Yang, J., Hu, G., Hu, Xi., Li, Z., Shen, S., Radosz, M. and Fan, M. (2016). Enhanced CO₂ capture capacity of nitrogen-doped biomass-derived porous carbons. *ACS Sustainable Chem. Eng.* 4: 1439–1445.
- Chen, L., Zhou, J., Zheng, X., Wu, J., Wu, X., Gao, X., Grehan, G. and Cen, K. (2017). Effects of carbon dioxide addition on the soot particle sizes in an ethylene/air flame. *Aerosol Air Qual. Res.* 17: 2522–2532.
- Chen, S., Cui, K., Zhu, J., Zhao, Y., Wang, L. and Mutuku, J. (2019). Effect of exhaust gas recirculation rate on the emissions of persistent organic pollutants from a diesel engine. *Aerosol Air Qual. Res.* 19: 812–819.
- Chew, T., Ahmad, A. and Bhatia, S. (2010). Ordered mesoporous silica (OMS) as an adsorbent and membrane for separation of carbon dioxide (CO₂). *Adv. Colloid Interface Sci.* 153: 43–57.
- Chi, T., Zuo, J. and Liu, F. (2017). Performance and mechanism for cadmium and lead adsorption from water and soil by corn straw biochar. *Front. Environ. Sci. Eng.* 11: 15.
- Ciuzas, D., Prasauskas, T., Krugly, E., Jurelionis, A., Seduikyte, L. and Martuzevicius, D. (2016). Indoor air quality management by combined ventilation and air cleaning: An experimental study. *Aerosol Air Qual. Res.* 16: 2550–2559.
- Fang, C., Zhang, Z., Jin, M., Zou, P. and Wang, J. (2017). Pollution characteristics of PM_{2.5} aerosol during haze periods in Changchun, China. *Aerosol Air Qual. Res.* 17: 888–895.
- Huang, J., Huang, Y., Lim, M., Zhang, J., Zhao, B., Jin, X. and Zhang, J. (2016). Emission characteristics and concentrations of gaseous pollutants in environmental moxa smoke. *Aerosol Air Qual. Res.* 16: 398–404.
- Huang, Y. and Wang, R. (2018). Review on fundamentals, preparations and applications of imprinted polymers. *Curr. Org. Chem.* 22: 1600–1618.
- Huang, Y. and Wang, R. (2019). Highly selective separation of H₂S and CO₂ using a H₂S-imprinted polymers loaded on a polyoxometalate@Zr-based metal-organic framework with a core-shell structure at ambient temperature. *J. Mater. Chem. A* 7: 12105-12114.
- Jain, A., Balasubramanian, R., Srinivasan, M. (2015). Production of high surface area mesoporous activated carbons from waste biomass using hydrogen peroxide-mediated hydrothermal treatment for adsorption applications. *Chem. Eng. J.* 273:622–629.
- Jiang, L., Gonzalez-Diaz, A., Ling-Chin, J., Roskilly, A.P. and Smallbone, A. (2019). Post-combustion CO₂ capture from a natural gas combined cycle power plant using activated carbon adsorption. *Appl. Energy* 245: 1–15.
- Kim, M., Sharma, P., Kim, Y., Fakhralam, S., Lee, H. and Cho, C. (2019). One-step template-free hydrothermal synthesis of partially Sr-incorporated hierarchical K-CHA zeolite microspheres. *Microporous Mesoporous Mater.* 286: 65–76.
- Kizito, S., Wu, S., Kirui, W., Lei, M., Lu, Q., Ba, H. and Dong, R. (2015). Evaluation of slow pyrolyzed wood and rice husks biochar for adsorption of ammonium nitrogen from piggery manure anaerobic digestate slurry. *Sci. Total Environ.* 505: 102–112.
- Lee, S. and Park, S. (2015). A review on solid adsorbents for carbon dioxide capture. *J. Ind. Eng. Chem.* 23: 1–11.

- Leung, D., Caramanna, G. and Maroto-Valer, M. (2014). An overview of current status of carbon dioxide capture and storage technologies. *Renewable Sustainable Energy Rev.* 39: 426–443.
- Li, B., Duan, Y., Luebke, D. and Morreale, B. (2013). Advances in CO₂ capture technology: A patent review. *Appl. Energy* 102: 1439–1447.
- Li, F., Yi, H., Tang, X., Ning, P., Yu, Q. and Kang, D. (2010). Adsorption of carbon dioxide by coconut activated carbon modified with Cu/Ce. *J. Rare Earths* 28: 334–337.
- Liu, H., Liu, C., Yang, X., Zeng, S., Xiong, Y. and Xu, W. (2008). Uniformly sized β -cyclodextrin molecularly imprinted microspheres prepared by a novel surface imprinting technique for ursolic acid. *Analytica Chimica Acta* 628: 87–94.
- Lu, C., Bai, H., Wu, B., Su, F. and Hwang, J. (2008). Comparative study of CO₂ capture by carbon nanotubes, activated carbons, and zeolites. *Energy Fuels* 22: 3050–3056.
- Martins, L., Hallak, R., Alves, R., Almeida, D., Squizzato, R., Moreira, C., Beal, A., Silva, I., Rudke, A. and Martins, J. (2018). Long-range transport of aerosols from biomass burning over southeastern South America and their implications on air quality. *Aerosol Air Qual. Res.* 18: 1734–1745.
- Merkel, T., Lin, H., Wei, X. and Baker, R. (2010). Power plant post-combustion carbon dioxide capture: An opportunity for membranes. *J. Membr. Sci.* 359: 126–139.
- Mohanty, P., Kull, L. and Landskron, K. (2011). Porous covalent electron-rich organonitridic frameworks as highly selective sorbents for methane and carbon dioxide. *Nat. Commun.* 2: 401.
- Nabavi, S., Vladisavljevic, G., VasilijeManovic, Y. (2017). Synthesis of size-tuneable CO₂-philic imprinted polymeric particles (MIPs) for low-pressure CO₂ capture using oil-in-oil suspension polymerisation. *Environ. Sci. Technol.* 51: 11476–11483.
- Naderi, S., Ahmadzadeh, H. and Goharshadi, E. (2019). Chemical capture of CO₂ by glycine salt solution. *Phys. Chem. Res.* 7: 765–774.
- Pan, J., Zou, X., Wang, X., Guan, W., Yan, Y. and Han, J. (2010). Selective recognition of 2,4-dichlorophenol from aqueous solution by uniformly sized molecularly imprinted microspheres with β -cyclodextrin/attapulgitic composites as support. *Chem. Eng. J.* 162: 910–918.
- Pan, S., Chiang, A., Chang, E., Lin, Y., Kim, H. and Chiang, P. (2015). An innovative approach to integrated carbon mineralization and waste utilization: A review. *Aerosol Air Qual. Res.* 15:1072-1091.
- Plaza, M., Pevida, C., Arenillas, A., Rubiera, F. and Pis, J. (2007). CO₂ capture by adsorption with nitrogen enriched carbons. *Fuel* 86: 2204–2212.
- Rojey, A. and Torp, T.A. (2005). Capture and geological storage of CO₂: An overview. *Oil Gas Sci. Technol.* 60: 445–448.
- Sahu, S. and Kota, S. (2017). Significance of PM_{2.5} air quality at the Indian capital. *Aerosol Air Qual. Res.* 17: 588–597.
- Sekiguchi, A., Shimadera, H. and Kondo, A. (2018). Impact of aerosol direct effect on wintertime PM_{2.5} simulated by an online coupled meteorology-air quality model over East Asia. *Aerosol Air Qual. Res.* 18: 1068–1079.
- Serafin, J., Baca, M., Biegun, M., Mijowska, E., Kaleńczuk, R.J., Sreńscek-Nazzal, J. and Michalkiewicz, B. (2019). Direct conversion of biomass to nanoporous activated biocarbons for high CO₂ adsorption and supercapacitor applications. *Appl. Surf. Sci.* 497: 143722.
- Shi, R., Hong, Z., Li, J., Jiang, J., Kamran, M., Xu, R. and Qian, W. (2018). Peanut straw biochar increases the resistance of two Ultisols derived from different parent materials to acidification: A mechanism study. *J. Environ. Manage.* 210: 171–179.
- Singh, G., Kim, I., Lakhi, K., Srivastava, P., Naidu, R. and Vinu, A. (2017). Single step synthesis of activated biocarbons with a high surface area and their excellent CO₂ adsorption capacity. *Carbon* 116: 448–455.
- Singh, G., Ismail, I., Bilen, C., Shanbhag, D., Sathish, C., Ramadass, K. and Vinu, A. (2019). A facile synthesis of activated porous carbon spheres from D-glucose using anon-corrosive activating agent for efficient carbon dioxide capture. *Appl. Energy* 255: 113831.
- Siriwardane, R., Shen, M., Fisher, E. and Poston, J. (2001). Adsorption of CO₂ on Molecular Sieves and Activated Carbon. *Energy Fuels* 15: 279–284.
- Thiruvenkatachari, R., Su, S., Yu, X. and Bae, J. (2013). Application of carbon fibre composites to CO₂ capture from flue gas. *Int. J. Greenhouse Gas Control.* 13: 191–200.
- Tsay, S., Maring, H., Lin, N., Buntoung, S., Chantara, S., Chuang, H., Gabriel, P., Goodloe, C., Holben, B., Hsiao, T., Hsu, N., Janjai, S., Lau W., Lee, C., Lee, J., Loftus, A., Nguyen, A., Nguyen, C., Pani, S., Pantina, P., Sayer, A., Tao, W., Wang, S., Welton, E., Wiriya, W. and Yen, M. (2016). Satellite-surface perspectives of air quality and aerosol-cloud effects on the environment: An overview of 7-SEAS/BASELInE. *Aerosol Air Qual. Res.* 16: 2581–2602.
- Wang, D., Gao, D., Huang, Y., Xu, W. and Xia, Z. (2019). Preparation of restricted access molecularly imprinted polymers based fiber for selective solid-phase microextraction of hesperetin and its metabolites in vivo. *Talanta* 202: 392–401.
- Wang, Y. and Li, N. (2010). Molecular imprinting technology and its application. *Chem. Ind. Eng. Prog.* 29: 2315–2323. (in Chinese with English Abstract)
- Wang, Q., Luo, J., Zhong, Z. and Borgna, A. (2011). CO₂ capture by solid adsorbents and their applications: Current status and new trends. *Energy Environ. Sci.* 4: 42–55.
- Wang, S., Yang, D. and Zeng, R. (2018). Immiscible multiphase flow behaviours of water-oil-CO₂ ternary system flooding using X-ray CT. *Aerosol Air Qual. Res.* 18: 1089–1101.
- Wickramaratne, N. and Jaroniec, M. (2013) Activated carbon spheres for CO₂ adsorption. *ACS Appl. Mater. Interfaces* 5: 1849–1855.
- Xie, W., Yu, M. and Wang R. (2017). CO₂ capture behaviors

- of amine-modified resorcinol-based carbon aerogels adsorbents. *Aerosol Air Qual. Res.* 17: 2715–2725.
- Xu, Z., Deng, P., Li, J., Tang, S. and Cui, Y. (2019). Modification of mesoporous silica with molecular imprinting technology: A facile strategy for achieving rapid and specific adsorption. *Mater. Sci. Eng., C* 94: 684–693.
- Yang, S., Zhan, L., Xu, X., Wang, Y., Ling, L. and Feng, X. (2013). Graphene-based porous silica sheets impregnated with polyethyleneimine for superior CO₂ capture. *Adv. Mater.* 25: 2130–2134.
- Yu, C., Huang, C. and Tan, C. (2012). A review of CO₂ capture by absorption and adsorption. *Aerosol Air Qual. Res.* 12: 745–769.
- Yu, K., Curcic, I., Gabriel, J. and Tsang, S. (2008). Recent advances in CO₂ capture and utilization. *ChemSusChem* 1: 893–899.
- Zhang, J., Burke, N., Zhang, S., Liu, K. and Pervukhina, M. (2014). Thermodynamic analysis of molecular simulations of CO₂ and CH₄ adsorption in FAU zeolites. *Chem. Eng. Sci.* 113: 54–61.
- Zhang, Z., Zhang, M., Liu, Y., Yang, X., Luo, L. and Yao, S. (2012). Preparation of L-phenylalanine imprinted polymer based on monodisperse hybrid silica microsphere and its application on chiral separation of phenylalanine racemates as HPLC stationary phase. *Sep. Purif. Technol.* 87: 142–148.
- Zhao, Y., Shen, Y., Ma, G. and Hao, R. (2014). Adsorption separation of carbon dioxide from flue gas by a molecularly imprinted adsorbent. *Environ. Sci. Technol.* 48: 1601–1608.

Received for review, October 6, 2019

Revised, December 17, 2019

Accepted, December 21, 2019